Manganese Cobalt Sulfide-Doped Fibrous Sulfurized Polyacrylonitrile for High-Rate and Long-Life Lithium-Sulfur Batteries

Jiayu Wang[a,b], Xiangyang Zhao[a,b], Qingli Zou[*c,b] and Min Wei[c,b]

[a]Beijing Key Laboratory of Electrochemical Process and Technology for Materials, Key Laboratory of Biomedical Materials of Natural Macromolecules, Ministry of Education

[b]Beijing University of Chemical Technology, Beijing 100029, People's Republic of China

[c]State Key Laboratory of Chemical Resource Engineering

Tab. S1 The elemental contents in the composites based on the elemental analysis.

Sample	S (%)	C (%)	N (%)	H (%)
FSPAN	44.51	39.89	14.18	1.61
MCS-FSPAN	45.27	39.97	14.37	0.45

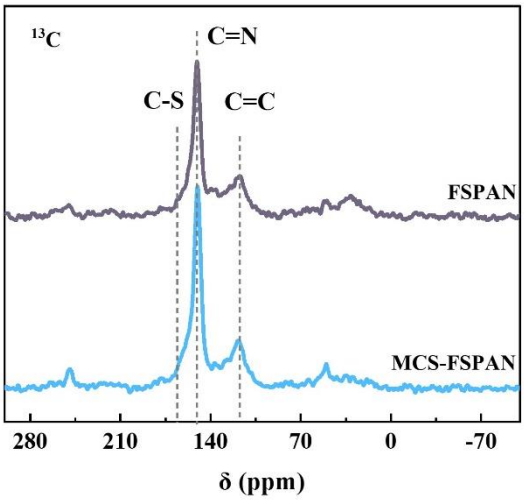

Fig. S1 ^{13}C NMR spectra of FSPAN and MCS-FSPAN

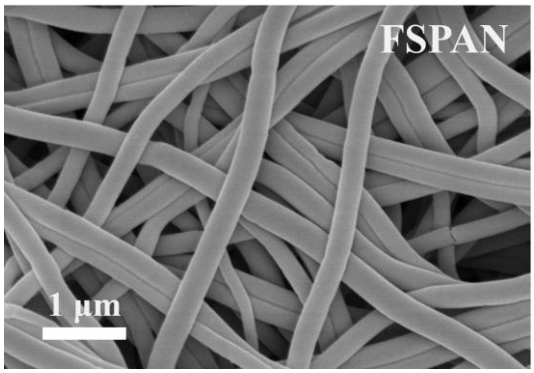

Fig. S2 Scanning electron microscopy images of FSPAN.

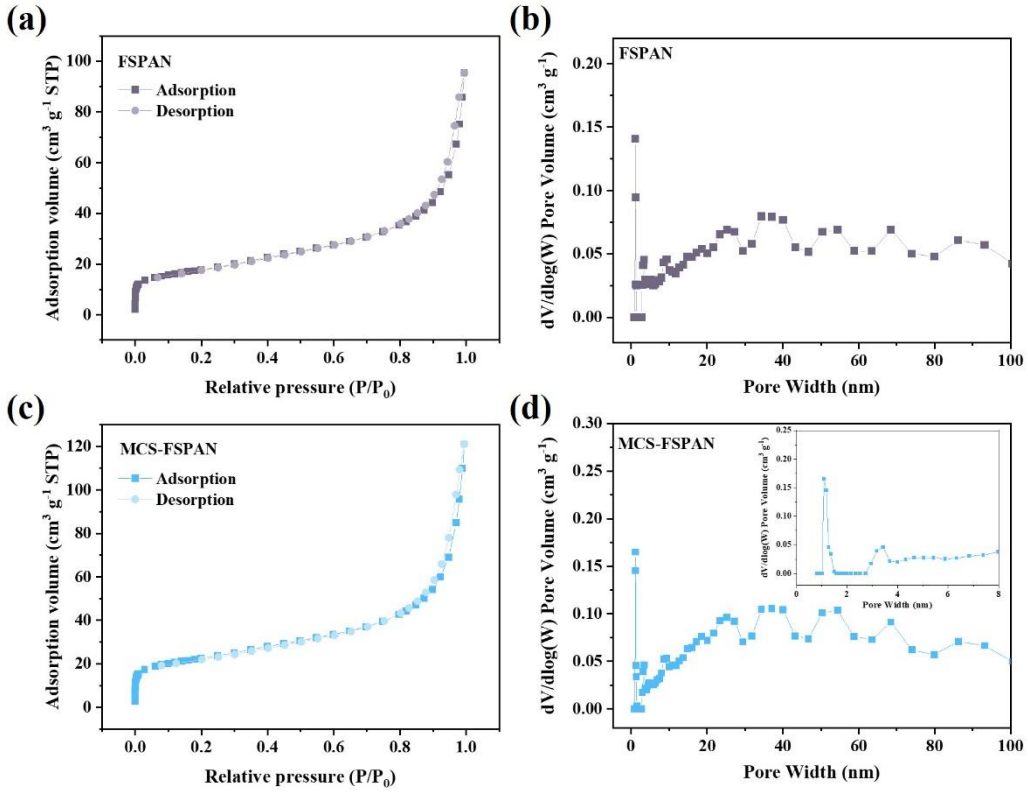

Fig. S3 (a) Nitrogen adsorption-desorption isotherm, (b) the corresponding DFT pore size distribution curve of FSPAN. (c) Nitrogen adsorption–desorption isotherm, (d) the corresponding DFT pore size distribution curve of MCS-FSPAN.

Tab. S2 Comparison of the surface area, pore volume for composites.

Material	Specific Surface Area (m^2 g^{-1})	Pore Volume (cm^3 g^{-1})
FSPAN	61.4	0.007
MCS-FSPAN	76.7	0.01

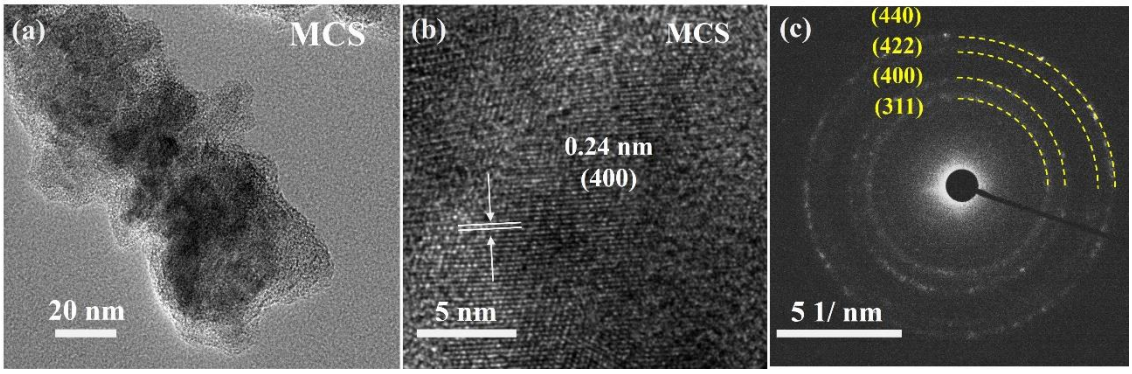

Fig. S4 (a) High-magnification TEM image of MCS, (b) HRTEM image and (c) the corresponding SAED pattern of MCS.

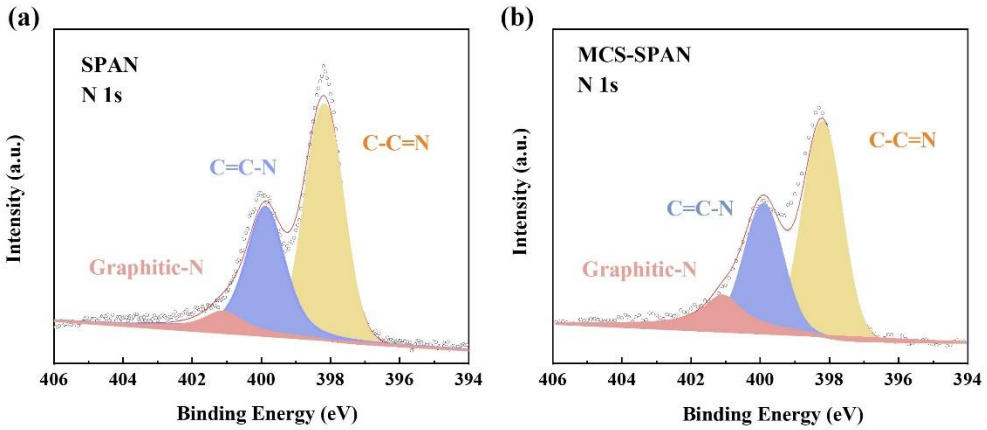

Fig. S5 N 1s XPS spectra of (a) SPAN and (b) MCS-SPAN.

Tab. S3 Electronic conductivity results of composites.

Sample	Conductivity (S m^{-1})
FSPAN	2.90×10^{-10}
MCS-FSPAN	5.12×10^{-10}

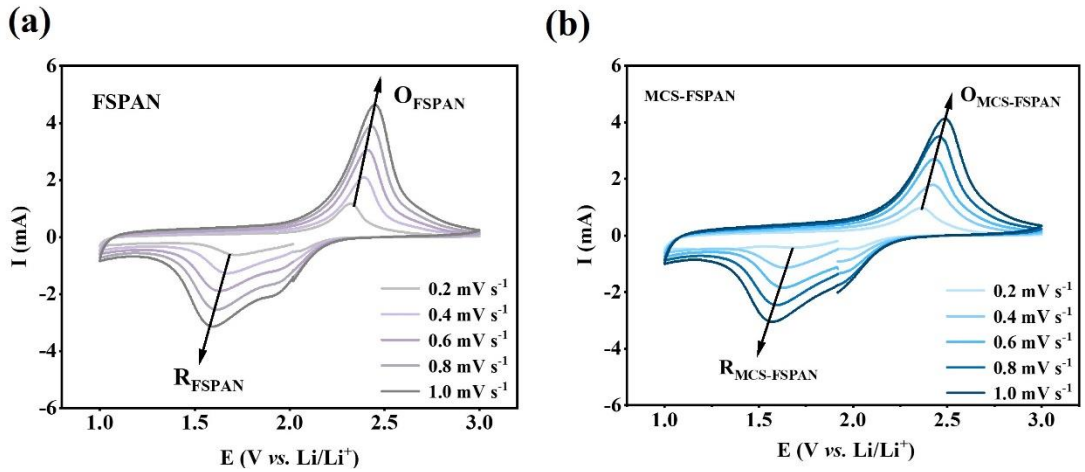

Fig. S6 CV curves of (a) FSPAN, (b) MCS-FSPAN at various scanning rates.

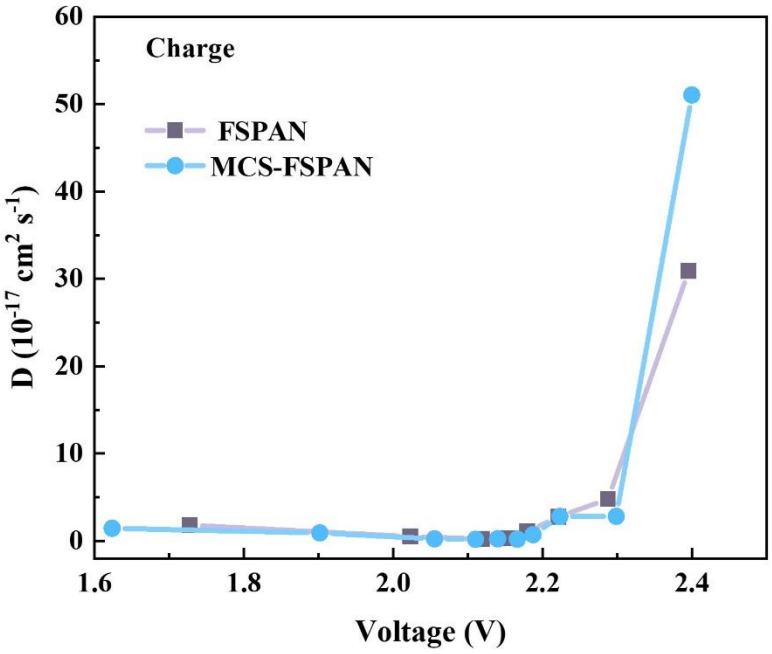

Fig. S7 Apparent diffusion coefficients calculated from the GITT potential profiles of FSPAN and MCS-FSPAN for charge during the first cycle.

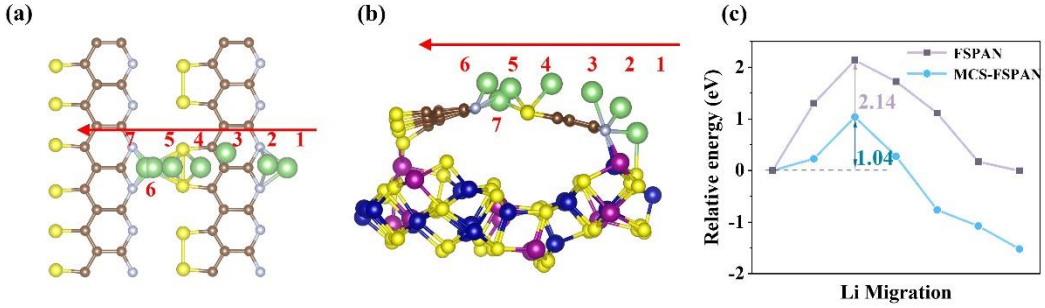

Fig. S8 (a) FSPAN and (b) MCS-FSPAN model for Li ion diffusion batteries employing DFT calculation, in which the diffusion path of lithium ion is marked as serial numbers. (c) Energy profiles for Li ion diffusion in FSPAN and MCS-FSPAN.

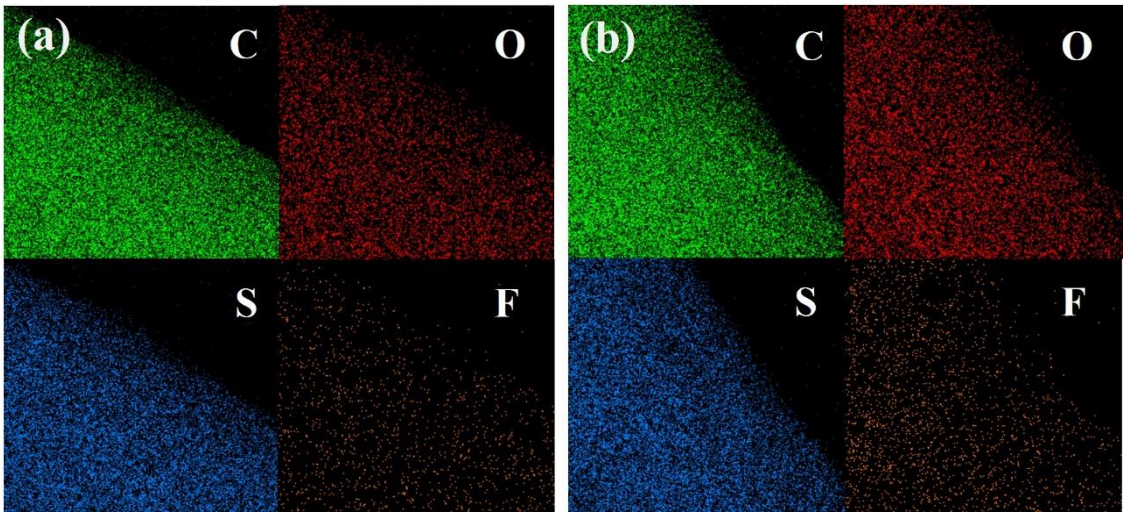

Fig. S9 EDS elemental mapping of (a) FSPAN and (b) MCS-FSPAN cathodes after cycled at 5 C current density.

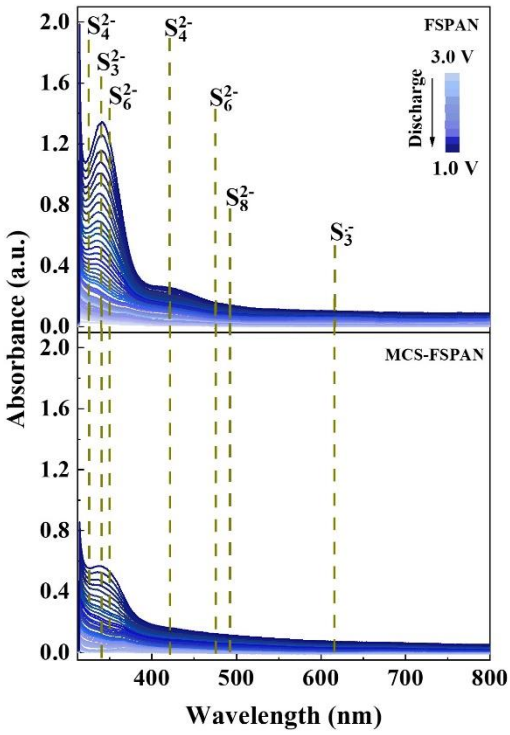

Fig. S10 In-situ UV-vis spectra of FSPAN and MCS-FSPAN electrodes cycled in conventional ether electrolyte.

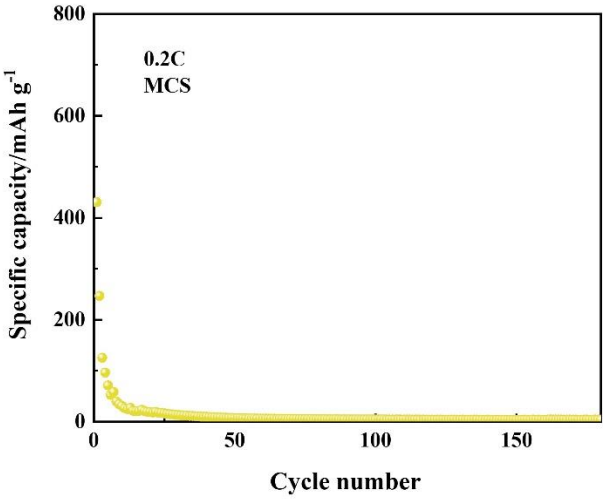

Fig. S11 Cycle performance of battery with MCS cathode at 0.2 C.

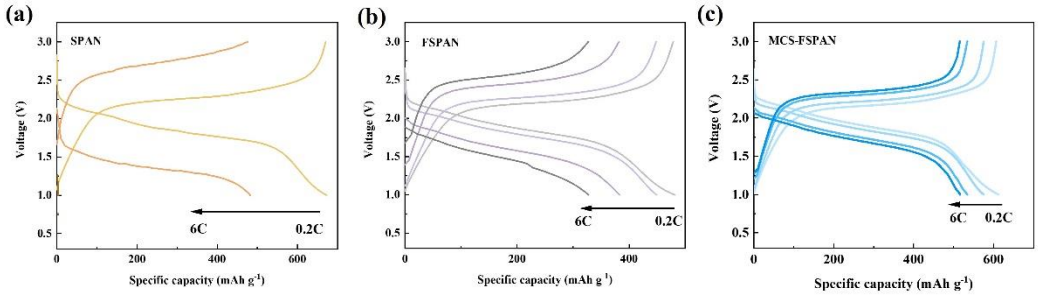

Fig. S12 Charge and discharge profiles of (a) SPAN, (b) FSPAN, (c) MCS-FSPAN at various current density.

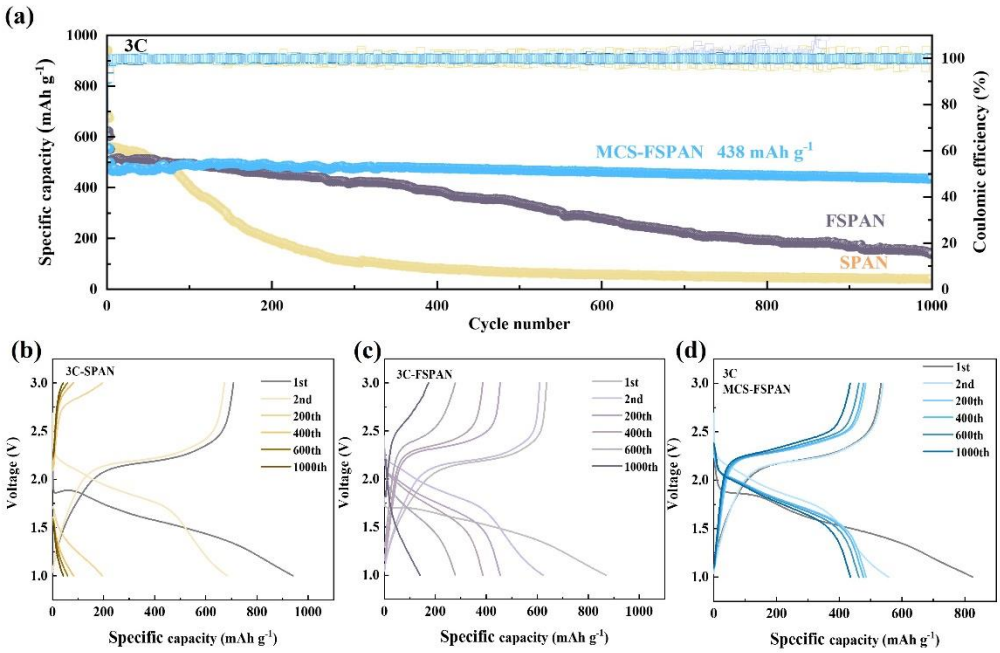

Fig. S13 (a) Long cycle performance of batteries with various cathodes at 3 C, and the corresponding Charge and discharge profiles of (b) SPAN, (c) FSPAN and (d) MCS-FSPAN.

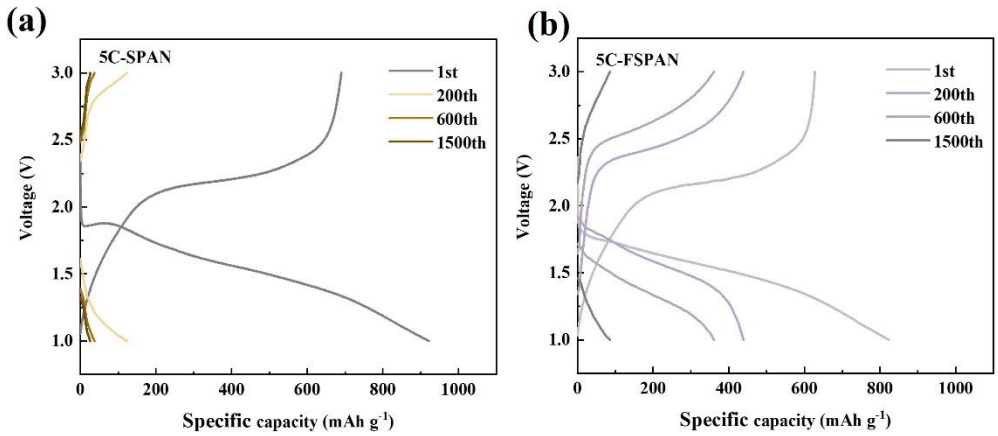

Fig. S14 Charge and discharge profiles of (a) SPAN, (b) FSPAN at 5 C.

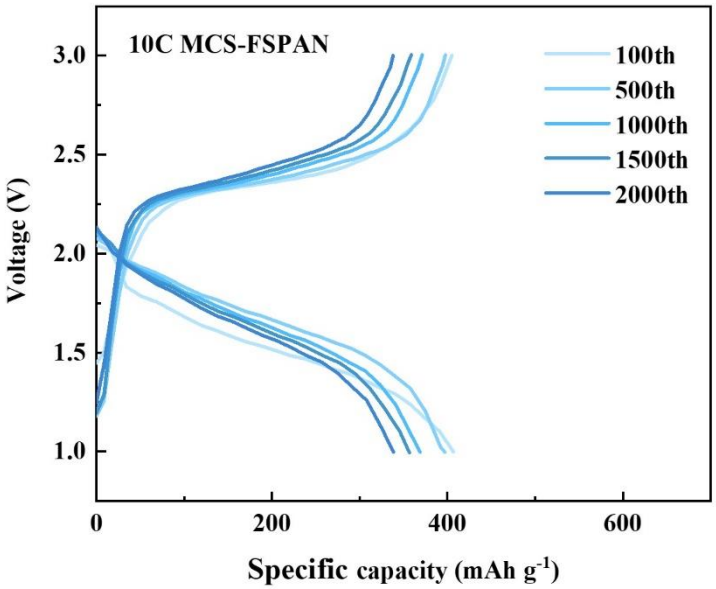

Fig. S15 Charge and discharge profiles of MCS-FSPAN at 10 C.

Tab. S4 Electrochemical performance of fibrous sulfurized polyacrylonitrile cathodes in lithium batteries

Cathode	Active material loading (mg cm^{-2})	Sulfur content (%)	Current density (A g^{-1})	Electrolyte/ sulfur (μL/mg)	Cycles	Specific capacity (mAh g^{-1} based on SPAN)	Fading rate (%)	Ref.
SPAN/CNT-12	2.0	41.02	0.8	30	800	484	/	[1]
H-SPAN	2.2	41.19	0.1675	44	300	509	/	[2]
SVF	6.4	37.78	3.35	26	300	227	/	[3]
SPAN-CNT20	0.9-1.1	40.30	1.675	149	500	442	/	[4]
SPAN/CNT	2.0	37.60	1	53	400	440	/	[5]
FeMn@GN-SPAN	3.0	33.20	0.5	15	500	280	0.025	[6]
C/S/PAN	/	53	0.2	/	400	390	/	[7]
SPANPPy-1%	1.5	43.3	1.675	20	500	368	/	[8]
porous PAN/S	/	48	3.34	/	500	381	0.10	[9]
$Se_{0.03}$SPAN/CNT-3	5.2	51.97	1.675	40	800	323	0.021	[10]
Co_{10}-SPAN-CNT	2.5	41.90	1.675	57	1500	427	0.012	[11]
I-SPAN	/	36.86	1	/	400	442	/	[12]
S@PAN/S_7Se	5.0	68	2	10-20	500	440	0.047	[13]
CoS_2-SPAN-CNT	2.4	43.20	1.675	24	400	380	/	[14]
MCS-FSPAN	1.0	41.33	3.0	145	1500	437	/	This work
			6.0	145	2000	338	0.01	

References

1. X. Wang, Y. Qian, L. Wang, H. Yang, H. Li, Y. Zhao and T. Liu, *Advanced Functional Materials*, 2019, **29**, 1902929.
2. X. Huang, J. Liu, Z. Huang, X. Ke, L. Liu, N. Wang, J. Liu, Z. Guo, Y. Yang and Z. Shi, *Electrochimica Acta*, 2020, **333**, 135493.
3. Y. Liu, A. K. Haridas, Y. Lee, K.-K. Cho and J.-H. Ahn, *Applied Surface Science*, 2019, **472**, 135-142.
4. A. Abdul Razzaq, Y. Yao, R. Shah, P. Qi, L. Miao, M. Chen, X. Zhao, Y. Peng and Z. Deng, *Energy Storage Materials*, 2019, **16**, 194-202.
5. W. X. Huilan Li, Lina Wang, Tianxi Liu, *ACS Appl Mater Interfaces*, 2021, **13**, 25002-25009.
6. B. Z. Xiaomin Yuan, Jinkui Feng, Chengguo Wang, Xun Cai, Rongman Qin, *ACS Appl Mater Interfaces*, 2021, **13**, 50936-50947.
7. J. Ye, F. He, J. Nie, Y. Cao, H. Yang and X. Ai, *Journal of Materials Chemistry A*, 2015, **3**, 7406-7412.
8. Y. Yi, F. Hai, J. Guo, X. Gao, W. Chen, X. Tian, W. Tang, W. Hua and M. Li, *Small*, 2023, **19**, 2303781.
9. K. Wang, S. Ju, Q. Gao, G. Xia, G. Wang, H. Yan, L. Dong, Z. Yang and X. Yu, *Journal of Alloys and Compounds*, 2021, **860**, 158445.
10. R. He, Y. Li, S. Wei, H. Liu, S. Zhang, N. Han, H. Liu, X. Wang and X. Zhang, *Journal of Alloys and Compounds*, 2022, **919**, 165838.
11. G. C. Amir Abdul Razzaq, Xiaohui Zhao, Xietao Yuan, Jiapeng Hu, Ziwei Li, Yufeng Chen, Jiabin Xu, Rahim Shah, Jun Zhong, Yang Peng, Zhao Deng, *Journal of Energy Chemistry*, 2021, **61**, 170-178.
12. W. X. Wenying Xue , Wei Wang , Guixia Gao , Lina Wang., *Composites Communications*, 2022, **30**, 101078.
13. B. He, Z. Rao, Z. Cheng, D. Liu, D. He, J. Chen, Z. Miao, L. Yuan, Z. Li and Y. Huang, *Advanced Energy Materials*, 2021, **11**, 2003690.
14. Y. X. Abdul Razzaq Amir, Chen Yujie, Hu Jiapeng, Mu Qiaoqiao, Ma Yong, Zhao Xiaohui, Miao Lixiao, Ahn Jou-Hyeon, Peng Yang, Deng Zhao, *Journal of Materials Chemistry A*, 2020, **8**, 1298-1306.